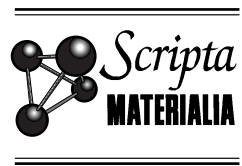




PERGAMON

Scripta mater. 44 (2001) 631–636



www.elsevier.com/locate/scriptamat

OBSERVATION OF LAMELLAR STRUCTURE IN A Zn-RICH Zn-6.3at.% Ag HYPER-PERITECTIC ALLOY PROCESSED BY RAPID SOLIDIFICATION

W. Xu¹, D. Ma¹, Y.P. Feng² and Y. Li¹

Departments of ¹Materials Science and ²Physics, Science Faculty, National University of Singapore, Singapore 119260, Singapore

(Received June 19, 2000)

(Accepted July 19, 2000)

Keywords: Zn-Ag alloy; Peritectic; Phase transformation; Microstructure; Rapid solidification

Introduction

According to the classical description, solidification of a peritectic alloy involves one solid phase reacting with a liquid phase on cooling to produce a second solid phase [1]. Recently, peritectic solidification has attracted more attention in experimental and theoretical studies [2–6]. The usual product of peritectic solidification is primary phase surrounded by peritectic phase and remaining liquid, due to the difficulty of diffusion in the solid primary phase. However, there are some reports on the possibility of coupled growth in peritectic systems [2,6–9]. In 1959, Chalmers [10] has suggested the possibility of simultaneous (coupled) growth of primary and peritectic phases in peritectic alloys if the growth of the primary phase can be suppressed by a high temperature gradient. In 1974, Flemings [11] also supported the idea of coupled growth in peritectic alloys. Later, however, Boettinger [2] solidified Sn-Cd alloys and predicted, by an analysis similar to the Jackson-Hunt theory [12] of lamellar eutectic growth, that coupled growth in peritectic systems was unstable. Laraia and Heuer [7] have suggested for some peritectic systems, particularly those in which the peritectic phase is a compound, that capillarity effects acting on the primary phase may lower its liquidus and promote a metastable eutectic reaction instead of the equilibrium peritectic reaction. Boettinger [13] has suggested that it may be possible to suppress the formation of the primary phase by applying rapid solidification. Based on this idea, rapid solidification by melt-spinning was carried out on a Zn-rich Zn-6.3at.(10 wt.%) Ag hyper-peritectic alloy and evidence of a resulting eutectic-like lamellar structure is reported. The possibility of coupled growth in the present peritectic system under rapid solidification conditions is also discussed.

Experimental

The Zn-6.3 at.% Ag alloy was prepared by melting pure 99.99% zinc and pure 99.99% silver in air in an induction furnace. Some 6–7 g of the as-cast ingot was melt-spun under argon from a quartz crucible on to a copper wheel at a speed of 20 m/s. The as-spun ribbons were typically 20–40 μm thick. Pieces of the as-spun ribbons were then heat treated at 423 K for 1.5 hours and 2 days respectively. The ribbons were examined in cross-section by scanning electron microscopy (SEM) and in the section parallel to

the ribbon plane by transmission electron microscopy (TEM) respectively. X-ray diffraction using CuK_α radiation was carried out on the chill and free sides of the ribbons. An image analyzer was employed for measuring the interphase spacing (λ) by a mean intercept method and the volume fractions of constituent phases on cross-sections. At least 20 readings were taken for each condition.

Results

A microstructure consisting of regular and degenerate lamellae, $\epsilon (\text{AgZn}_3) + \eta (\text{Zn})$, was observed in the cross-section of the as-spun ribbons, as shown in Fig. 1(a), in which regular lamellar colonies are embedded in a matrix of the degenerate lamellae. The regular colonies are several microns in size and there are no clear boundaries between regular colonies and the degenerate lamellae. The lamellar spacing has been measured in the regular colonies, giving a value of $0.36 \pm 0.07 \mu\text{m}$. The volume fraction of the ϵ phase (bright phase) has been measured as about 0.4~0.6. Figs. 1 (b) and (c) show coarsened lamellar structures in the ribbons heat-treated at 423 K for 1.5 hours and 2 days respectively. The resultant lamellar spacings of $0.56 \pm 0.14 \mu\text{m}$ and $0.85 \pm 0.17 \mu\text{m}$ are typically 1.5 and 2 times that of the as-spun ribbon. Fig. 2 shows a TEM micrograph of a section parallel to the ribbon plane of the as-spun ribbon, showing lamellar structure of ϵ and η phases. Selected-area diffraction patterns from the bright phase η (upper) and dark phase ϵ (lower) in Fig. 2 show that the two phases have similar crystal structures and lattice parameters. X-ray diffraction on both chill and free sides of as-spun ribbons give the same result. The result for the chill side is shown in Fig. 3, indicating presence of ϵ and η phases.

Discussion

Unlike the situation for eutectic systems, few studies have been carried out to investigate microstructure evolution in peritectic systems under rapidly directional solidification conditions except for two detailed investigations [14,15]. For a melt-spun Mg-rich Mg-2.0 wt.%Mn peritectic alloy Skjerpe [14] showed a cellular structure with a cell spacing of 1~2 μm and an intercellular region enriched with Mn. Melt-spun Ti-Al peritectic alloys showed metastable phases [15], including equiaxed $\alpha_2\text{-Ti}_3\text{Al}$, two-phase $\alpha_2\text{-Ti}_3\text{Al}$ (particles) + $\gamma\text{-TiAl}$, single-phase $\gamma\text{-TiAl}$ and two-phase $\alpha_2 + \gamma$ in a cellular morphology, depending on alloy compositions. However, neither study reported coupled growth under the rapid solidification conditions employed.

The rapid solidification of the present Zn-6.3 at% Ag hyper-peritectic alloy has given a structure with regular lamellar colonies embedded in a matrix of the degenerate lamellae. The usual peritectic microstructure of primary ϵ surrounded by peritectic η was not observed in the as-spun ribbons. The microstructure in Figs. 1 and 2 instead strongly resembles the eutectic lamellar structure observed in Al-CuAl₂ eutectic alloy rapidly solidified by melt-spinning [16]. We have termed the present structure eutectic-like lamellar rather than plate-like cellular, because (i) the similarity in morphology between present structure and eutectic lamellar structure; (ii) the volume fraction of the ϵ phase is about 0.4~0.6, which falls in the typical range of 0.28~.5 for lamellar eutectic formation [17]; (iii) the resultant structure (Figs. 1 (b) and (c)) after heat treatment also resembles that of the eutectic lamellar structure, indicating coarsening of the lamellar spacing with increase of heat-treatment temperature and time; (iv) TEM and XRD evidently show two phases present.

Lee and Verhoeven [6] have reported cellular coupled growth of γ and γ' phases in directional solidification of Ni-Al peritectic alloys at high G/V conditions sufficient to give plane front growth, giving a cell spacing of about 30 μm . Busse and Meissen [8] have observed a eutectic-like lamellar structure with a spacing of 30 μm in TiAl with 53.4 at.% Al directionally solidified at a very low growth

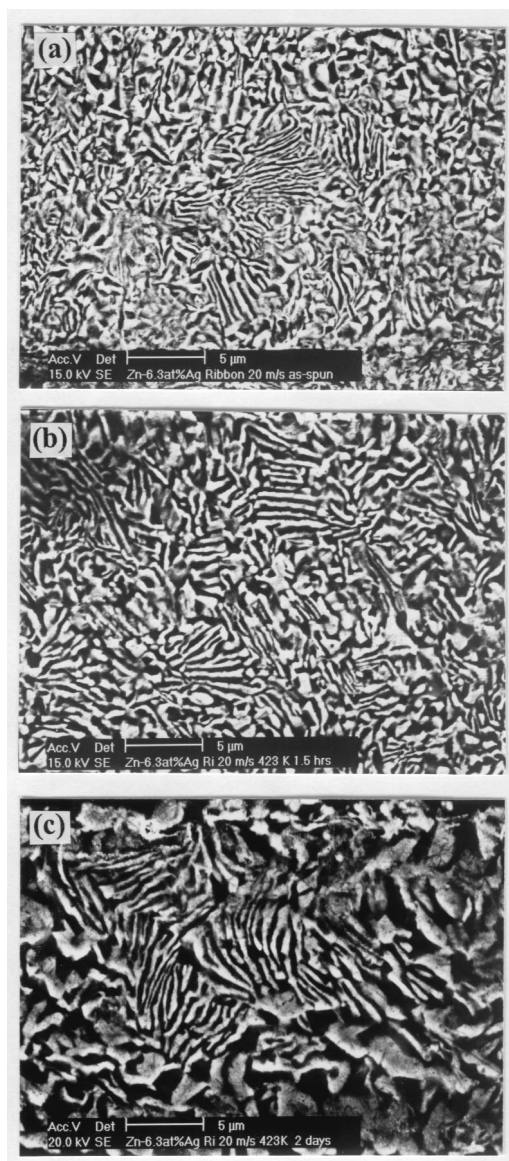


Figure 1. SEM micrographs of melt-spun ribbons of Zn-6.3 at.% Ag hyper-peritectic alloy: (a) as-spun, (b, c) heat-treated at 423 K for (b) 1.5 hours and (c) 2 days.

velocity of $0.83 \mu\text{m/s}$. Recently Vandyoussefi et al [9] have shown coupled growth in a Fe-4.49 at.% Ni peritectic alloy at growth velocities of 10 to $15 \mu\text{m/s}$ with an interphase spacing of about $80 \mu\text{m}$. Their results have indicated an instability of the coupled growth with increase in volume fraction of peritectic phase (γ) [9]. It is noted that the observed interphase spacings in the three investigations [6,8,9] are very large, typically one order of magnitude larger than for eutectic systems at similar growth conditions.

However, our present study has shown two key differences from the above-mentioned observations [6,8,9], i.e. (i) the ratio of the volume fractions of ϵ and η phases in present study is about unity whereas

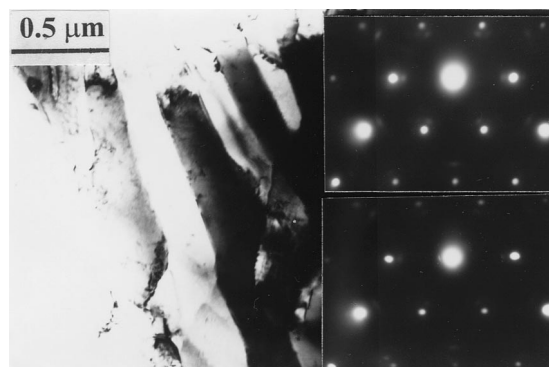


Figure 2. TEM micrograph showing lamellar $\eta + \epsilon$ structure in a section parallel to the ribbon plane in as-spun ribbon of the Zn-6.3 at.%Ag hyper-peritectic alloy.

the volume fractions of the peritectic phases in both Ni-Al [6] and Fe-Ni [9] peritectic systems are very small; (ii) the growth condition is one of rapid solidification for the present study compared with directional solidification at lower velocities (or higher G/V values) for the investigations on Ni-Al [6], Ti-Al [8] and Fe-Ni [9] peritectic systems. On the other hand, the lamellar spacing in our as-spun sample, $0.36 \mu\text{m}$, is also much larger than that of 18 nm for the Al-Cu eutectic system [18] under rapid solidification conditions. It seems to indicate coupled growth in peritectic systems will give a larger interphase spacing than that in eutectic systems.

Plane front growth is stable at growth velocities below V_c (the limit of constitutional undercooling) or above $V_a (= \Delta T_0 D / k \Gamma)$, the limit of absolute stability, where ΔT_0 is the liquidus-solidus range at C_0 , D is the diffusion coefficient in the liquid, k is the distribution coefficient and Γ is Gibbs-Thomson coefficient) [1]. Vandyoussefi et al [9] have assumed that coupled growth in the Fe-Ni peritectic alloy occurs preferentially at velocities smaller than V_c . However, the results of the present study suggest that coupled growth in peritectic alloys might also take place under rapid solidification with a growth velocity above V_a . For present study, the value of V_a was calculated to be 0.42 m/s ($\Delta T_0 = 113 \text{ K}$, $k = 5.67$, $D = 2.31 \times 10^{-3} \text{ mm}^2$ [19] and $\Gamma = 1.1 \times 10^{-4} \text{ K}\cdot\text{mm}$ [20]), which is close to the estimated maximum growth velocity, 0.3 m/s , for pure Zn and dilute Zn alloys during melt spinning [21].

One reason for the formation of a eutectic-like lamellar structure in the present study is probably the conversion of the equilibrium peritectic reaction into a metastable eutectic reaction under rapid solidification conditions, as shown in Fig. 4. According to Perepezko and Boettinger [22], for rapid solidification phase diagrams should have an important role in the interpretation of possible product phases and solidification paths. In this case the liquidus, solidus, partition coefficient or other

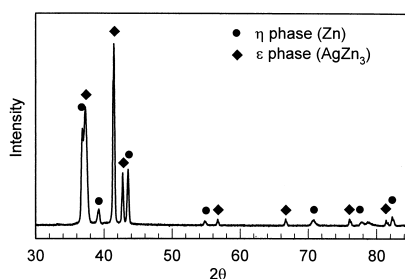


Figure 3. Result of X-ray diffraction for the chill side of as-spun ribbon of Zn-6.3 at.%Ag hyper-peritectic alloy.

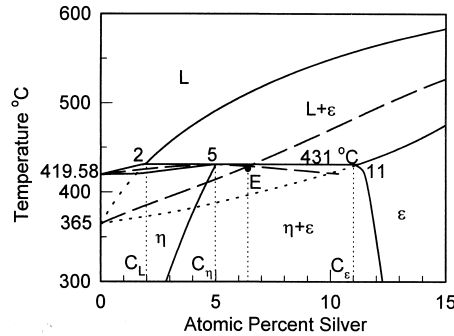


Figure 4. Binary equilibrium phase diagram of Zn-rich Zn-Ag alloys (redrawn from Ref. [25]). Dashed lines show the hypothetical conversion of the equilibrium peritectic reaction into a metastable eutectic reaction under rapid solidification conditions. The metastable ϵ -liquidus and η -liquidus lines intersect at E.

thermodynamic data for a metastable phase are important. The dependence of the liquidus slope on the growth velocity was given by Boettinger and Coriell [23]

$$m_v^i = \frac{1 - k_v^i [1 - \ln(k_v^i/k_e^i)]}{1 - k_e^i} m_e^i \quad (1)$$

as where k_e^i is the equilibrium distribution coefficient and k_v^i the non-equilibrium distribution coefficient defined by Aziz [24] to be

$$k_v^i = \frac{k_e^i + V/V_D}{1 + V/V_D} \quad (2)$$

where $V_D (= D_i/a_0)$ is the diffusion rate through the interface, D_i the solute diffusion coefficient across the interface, and a_0 a distance of the order of the thickness of the interface.

For the present study, the thermodynamic data obtained from the equilibrium Zn-Ag phase diagram [25] are $k_e^\epsilon = 5.67$, $k_e^\eta = 2.67$, $m_e^\epsilon = 10.8$ and $m_e^\eta = 3.8$, where ϵ is the primary phase and η is the peritectic phase. From equations (1) and (2), as the growth velocity increases, both k_v^ϵ and k_v^η tend to unity and both m_v^ϵ and m_v^η decrease. In Fig. 4 the liquidus of ϵ is shifted to the right and downward due to high growth velocity and capillarity effects [7]. The decrease of the liquidus slopes possibly meets the requirement for the formation of a metastable eutectic point (E in Fig. 4), i.e., an azeotrope point or maximum in the metastable extension will result if the liquidus slope of η is approximately horizontal. Obviously this conversion requires a high growth velocity, which could be obtained in the melt-spun ribbons.

Finally, for pure Zn and dilute Zn alloys during melt spinning, Akdeniz and Wood [21] have estimated the average growth velocity as 0.1 m/s and the maximum as 0.3 m/s for the initial stage. It is reasonable for us to choose the range 0.1~0.3 m/s as the approximate growth velocities for the present melt-spun ribbons. The consequential value of $\lambda V^{1/2}$ for this alloy is about 114~197 $\mu\text{m}^{3/2} \text{s}^{-1/2}$, which is much higher than that of 9.4 $\mu\text{m}^{3/2} \text{s}^{-1/2}$ for rapidly solidified Al-Cu hypereutectic alloys [18]. This estimated value of $\lambda V^{1/2}$ is also larger than the values of 27 $\mu\text{m}^{3/2} \text{s}^{-1/2}$ for the Ti-Al [8] peritectic alloy and 45 $\mu\text{m}^{3/2} \text{s}^{-1/2}$ for Ni-Al peritectic alloys [6] but comparable with that of 252 $\mu\text{m}^{3/2} \text{s}^{-1/2}$ for the Fe-Ni [9] peritectic alloy.

Conclusions

Eutectic-like lamellar structure consisting of two phases ($\eta + \epsilon$) has been observed in as-spun ribbons of a Zn-rich Zn-6.3at.%Ag hyper-peritectic alloy. Coupled growth has been suggested to take place under rapid solidification conditions with a growth velocity above that for absolute stability. A qualitative analysis indicates that the formation of the eutectic-like lamellar structure is possibly ascribed to the conversion of the equilibrium peritectic reaction into a metastable eutectic reaction under sufficiently rapid solidification conditions.

Acknowledgments

The authors wish to thank Prof. H. Jones for his critical comments on our manuscript.

References

1. H. W. Kerr and W. Kurz, *Int. Mater. Rev.* 41, 129 (1996).
2. W. J. Boettinger, *Metall. Trans.* 5, 2023 (1974).
3. W. Kurz and R. Trivedi, *Metall. Mater. Trans.* 22A, 625 (1996).
4. D. Ma, Y. Li, S. C. Ng, and H. Jones, *Acta Mater.* 48, 419 (2000).
5. D. Ma, Y. Li, S. C. Ng, and H. Jones, *Acta Mater.* 48, 1741 (2000).
6. J. H. Lee and J. D. Verhoeven, *J. Crystall. Growth.* 144, 353 (1994).
7. V. J. Lariaia and A. H. Heuer, *Scripta Metall. Mater.* 25, 2803 (1991).
8. P. Busse and F. Meissen, *Scripta Mater.* 36, 653 (1997).
9. M. Vandyoussefi, H. W. Kerr, and W. Kurz, *Acta Mater.* 48, 2297 (2000).
10. B. Chalmers, *Physical Metallurgy*, pp. 271–272, Wiley, New York (1959).
11. M. C. Flemings, *Solidification Processing*, pp. 177–180, McGraw-Hill, New York (1974).
12. K. A. Jackson and J. D. Hunt, *Trans. Am. Inst. Miner. Eng.* 236, 1129 (1966).
13. W. J. Boettinger, in *Rapidly Solidified Amorphous and Crystalline Alloys*, ed. B. H. Kear, B. C. Giessen, and M. Cohen, *Materials Research Society Symposia Proc.*, vol. 8, p. 15 (1982).
14. P. Skjerpe, *Mater. Sci. Technol.* 1, 316 (1985).
15. E. L. Hall and S. C. Huang, *Acta Metall. Mater.* 38, 539 (1990).
16. D. B. Williams and J. W. Edington, *J. Mater. Sci.* 12, 126 (1977).
17. W. Kurz and D. J. Fisher, *Fundamentals of Solidification*, Trans Tech Publishers, Zurich, Switzerland (1992).
18. S. C. Gill and W. Kurz, *Acta Metall. Mater.* 41, 3563 (1993).
19. I. I. Tychina and T. V. Vasilenko, *Izv. Akad. Nauk SSSR Metal.* 4, 101 (1972).
20. H. Y. Liu and H. Jones, *Acta Metall.* 40, 229 (1992).
21. M. V. Akdeniz and J. V. Wood, *J. Mater. Sci.* 31, 545 (1996).
22. J. H. Perepezko and W. J. Boettinger, *Mater. Res. Soc. Symp. Proc.* 19, 223 (1983).
23. W. Boettinger and S. R. Coriell, in *Science and Technology of the Undercooled Melt*, NATO ASI Series E, No. 114, ed. P. R. Sahm, et al., pp. 81–108, Martinus Nijhoff, Dordrecht (1986).
24. M. J. Aziz, *J. Appl. Phys.*, 53, 1158 (1982).
25. T. B. Massalski, *Binary Alloy Phase Diagrams*, American Society for Metals (1986).